Fluid mechanical modelling of the scroll compressor

by
Peter Howell
University of Oxford

Mathematical Institute, 24–29 St Giles', Oxford OX1 3LB, UK

Preface. This case-study concerns the flow of gas in a so-called *Scroll Compressor*. In this device a number of chambers of gas at different temperatures and pressures are separated by narrow channels through which leakage can occur. Using compressible lubrication theory, an estimate for the leakage rate is found in terms of the material properties of the gas and the geometry of the compressor. Thus a simple functional is obtained which allows the efficiency of different compressor designs to be compared. Next we derive a set of ordinary differential equations for the temperature and pressure in each chamber; the coupling between them arises from the leakage. The numerical solution of these equations allows a realistic simulation of a working compressor, and suggests some interesting possibilities for future designs.

This problem arose at the *32nd European Study Group with Industry* held in September 1998 at the Technical University of Denmark — the first ever to be held outside the United Kingdom. It was presented by Stig Helmer Jørgensen from DANFOSS, which is Denmark's largest industrial group and specialises in controls for refrigeration and heating. The Danish Study Group was a great success and is expected to be repeated annually henceforth. The feedback from DANFOSS has also been encouraging and hopefully this represents the start of a long-term collaboration.

1 Introduction

The scroll compressor is an ingenious machine used for compressing air or refrigerant, which was originally invented in 1905 by Creux [1]. Unfortunately, technology was insufficiently advanced at the time for workable models to be manufactured and it wasn't until the 1970's that commercial interest in the idea was revived — see *e.g.* [3]. The device consists of two nested identical scrolls, one of which is rotated through 180° with respect to the other. In the classical design, both scrolls are *circle involutes* as shown in figure 1. Now, while the darker scroll is held fixed the other is moved through a clockwise circular motion such that the two always remain in contact, going successively through the positions shown in diagrams A, B, C, and D of figure 1. Each scroll is fitted to a backplate so that a side view looks something like figure 2: the top diagram is for a section in which the scrolls are in contact and the bottom one for any other section. Notice the gaps at the sides where gas can be ingested and the outlet gap in the middle.

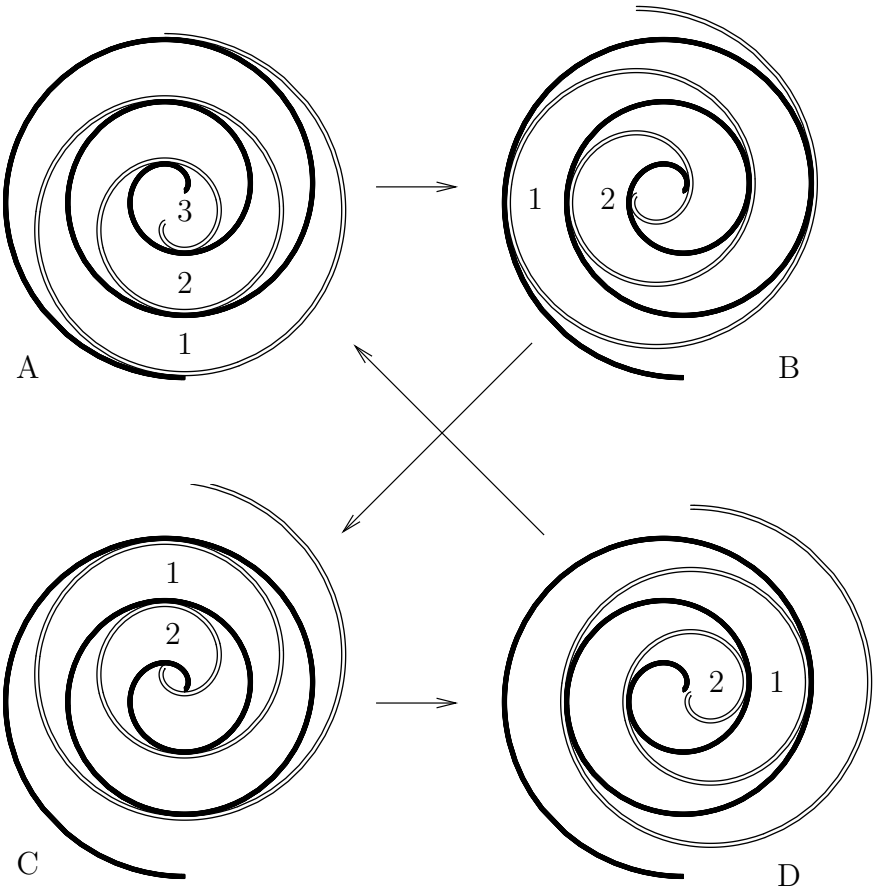

Figure 1: Schematic diagram of a scroll compressor

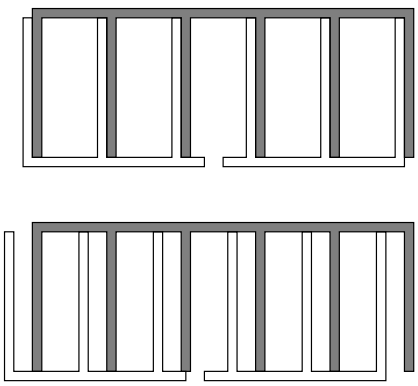

Figure 2: Side view of a scroll compressor

To see how the compressor works, consider first the pocket of gas marked "1" in diagram A of figure 1. This has just been ingested from the gas outside the scrolls and is now sealed inside what we shall henceforth call a "chamber". After one quarter of a cycle we move to diagram B and find that chamber 1 has rotated clockwise and decreased in size; this continues through diagrams C and D. Then, after one complete cycle we are back at diagram A, but the gas that started life in chamber 1 is now in chamber 2. As we continue through the second cycle, chamber 2 is compressed further and finally, at the beginning of the third cycle, it turns into chamber 3 which now opens up to a vent at the centre of the scroll through which the compressed gas escapes.

Today, scroll compressors are widely used for compressing refrigerants in air-conditioners and industrial refrigerators, and somewhat less widely for air compression. There are many advantages over the traditional pump-type design. For example, only a small number of moving parts and no valves are required, and the rotary motion can be completely balanced, reducing vibration and noise. The biggest problem with them is leakage of gas, resulting in reduced efficiency, and when possible new designs are considered, controlling the leakage is of paramount importance.

Another problem with the traditional design is that the compression takes place rather slowly, so that a large number of turns is required to achieve the high compression ratios demanded by customers. Unfortunately, for a given total cross-sectional area, increasing the tightness of the spiral (*i*) decreases the "choke volume" of gas that can be ingested in each cycle (*i.e.* the volume of chamber 1 in figure 1A), (*ii*) makes the job of machining the scrolls more difficult, and (*iii*) increases the rate of leakage. A possible solution to this problem is to use a different spiral from the circle involute shown in figure 1, specifically one that gives more rapid compression without reducing the intake volume.

The questions asked of the Study Group by DANFOSS were:

Q1. What different spiral geometries can be used to make a workable scroll compressor?

Q2. How do different scroll geometries affect the performance and efficiency of the compressor?

Q3. Can we devise a "cost-function" that can be used to optimise over different proposed designs?

The problem divides naturally into two lines of attack. First, it is an exercise in the geometry of plane curves to determine the important characteristics (choke volume, compression ratio, *etc.*) of a compressor made from a given spiral. Second, once these geometrical properties have been determined, the performance and efficiency must be found by considering the fluid mechanics of the gas. It is the second aspect of the problem (*i.e.* questions 2 and 3) that is the subject of this case study. We will suppose that the chamber volumes and all other important geometrical parameters are known, and attempt to assess their effects on the behaviour of the gas in the compressor. For more details about the geometrical aspects of the problem, see the Study Group Report [2]. (It was found that the important properties of a compressor design are conveniently found by expressing the spirals in the "natural" arc-length/angle formulation.)

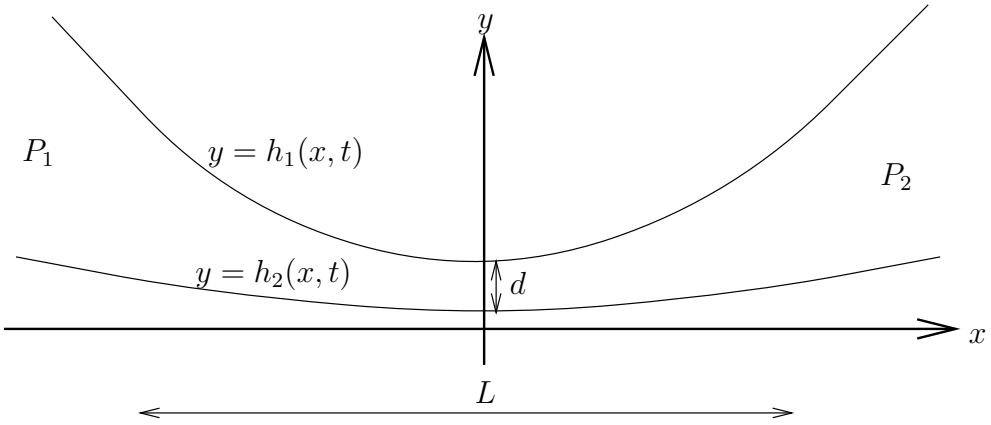

Figure 3: Schematic diagram of the gap between two chambers.

The first consideration is the leakage between adjoining chambers, which forms the subject of section 2. Then in section 3 we derive equations for the temperature and pressure of the gas in each chamber. The leakage found in section 2 acts as a coupling mechanism between a chamber and its neighbours, and a fully coupled model is described in section 4. Some numerical results for a simple realisation of this model are presented in section 5 and the conclusions are drawn in section 6, where some further projects for the interested reader are also suggested.

2 Leakage between chambers

Ideally, the two halves of a scroll compressor remain perfectly in contact as they rotate. In reality it is not practical to machine them accurately enough for this to be the case, and instead there is a narrow gap. Typically the gap is around one micron across; this may be increased by wear and/or poor machining, and it is known that if it reaches around eight microns, the compressor becomes useless. In this section we analyse the flow through this gap in an attempt to determine the leakage between neighbouring chambers in the compressor. A schematic diagram of the geometry is given in figure 3. Here a gap of typical thickness d and length L separates two adjacent chambers containing gas at pressures P_1 and P_2. The lengthscale L appears to be somewhat arbitrary; a typical value of 1 cm was obtained by "eyeballing" a sample compressor (whose total diameter was of the order of 20 cm) supplied by DANFOSS.

A local coordinate system is adopted with x pointing along the gap and y pointing across it. With respect to these coordinates we denote the bottom and top scroll walls (both of which are moving as the compressor rotates) by $y = h_1(x,t)$ and $y = h_2(x,t)$.

2.1 Governing equations and boundary conditions

The governing equations for the flow are the compressible Navier-Stokes equations (see [4])

$$\rho_t + \mathrm{div}(\rho \boldsymbol{u}) = 0, \tag{1}$$

$$\rho\frac{D\boldsymbol{u}}{Dt} = -\text{grad}\, p + (\lambda+\mu)\text{grad}\,\text{div}\,\boldsymbol{u} + \mu\nabla^2\boldsymbol{u}, \tag{2}$$

where ρ, $\boldsymbol{u}$ and p are the density, velocity and pressure fields, λ and μ are the dilatational and shear viscosities, and D/Dt is the usual convective derivative. Equation (1) represents conservation of mass, and must be satisfied by *any* continuum with velocity $\boldsymbol{u}$ and density ρ, while (2) is the generalisation of the usual incompressible Navier-Stokes equation, which is recovered if $\text{div}\,\boldsymbol{u}$ is set to zero.

In contrast with the incompressible case, (1, 2) is *not* a closed system since the unknowns ρ, $\boldsymbol{u}$ and p outnumber the equations by one. Thus it is necessary to consider also the *energy equation* (see [4])

$$\rho c_v\frac{DT}{Dt} + p\,\text{div}\,\boldsymbol{u} = k\nabla^2 T + \Phi, \tag{3}$$

where T is absolute temperature, k and c_v are the thermal diffusivity and specific heat at constant volume of the gas, and Φ is the *dissipation*, given by

$$\Phi = \lambda(\text{div}\,\boldsymbol{u})^2 + \frac{\mu}{2}\left(\frac{\partial u_i}{\partial x_j} + \frac{\partial u_j}{\partial x_i}\right)^2. \tag{4}$$

The terms in (3) represent respectively (i) rate of change of thermal energy, (ii) work done by pressure, (iii) diffusion of heat and (iv) heat generated by viscous effects.

Finally, the system is closed by specifying an equation of state. Treating the air as a perfect gas, we set

$$p = \rho RT, \tag{5}$$

where the so-called gas constant R can be written as

$$R = c_p - c_v,$$

and c_p is the specific heat at constant pressure. It is convenient to substitute (1) and (5) into the left-hand side of (3) to obtain the energy equation in the form

$$\frac{1}{\gamma-1}\frac{Dp}{Dt} - \frac{\gamma}{\gamma-1}\frac{p}{\rho}\frac{D\rho}{Dt} = k\nabla^2 T + \Phi, \tag{6}$$

where γ is the ratio of specific heats,

$$\gamma = \frac{c_p}{c_v},$$

which takes a value very close to 1.4 for air.

As an aside we note that in many gas dynamics problems the right-hand side of (6) is negligible compared with the left-hand side. If so, (6) implies that $D/Dt(p/\rho^\gamma) = 0$, and often one can deduce further that p is given as a function of density by $p = k\rho^\gamma$ for some constant k; such flows are described as *homentropic*. This approach does not work for the current problem since we will find that the dissipation term on the right-hand side of (6) is necessarily the same order as the left-hand side.

On the upper and lower walls we specify the velocity $\boldsymbol{u} = (u, v)$ of the gas to be the same as that of the scroll:

$$u = u_i, \quad v = \frac{\partial h_i}{\partial t} + u_i\frac{\partial h_i}{\partial x}, \quad \text{on } y = h_i(x,t); \quad i = 1, 2. \tag{7}$$

Property	Symbol	Approx. value	Units
Viscosity	μ	10^{-5}	$\mathrm{Pa\,s}$
Density	$\bar{\rho}$	1	$\mathrm{Kg\,m^{-3}}$
Thermal diffusivity	k	2.5×10^{-2}	$\mathrm{J\,m^{-1}s^{-1}K^{-1}}$
Specific heat	c_v	10^3	$\mathrm{J\,Kg^{-1}K^{-1}}$
Gap thickness	d	10^{-6}	m
Contact length	L	10^{-2}	m
Rotation frequency	ω	50	$\mathrm{s^{-1}}$
Pressure drop	ΔP	10^6	Pa

Table 1: Estimated parameter values for leakage between chambers in a scroll compressor

Here the horizontal velocity u_i and position h_i of each wall are determined by the prescribed shape and motion of the scroll. Note that (7) holds for *any* such motion, even if the walls were flexible (*e.g.* peristaltic action), although only rigid walls are relevant to our application.

We now integrate (1) with respect to y and apply the boundary conditions (7) to obtain an integrated equation representing total conservation of mass:

$$m_t + q_x = 0, \quad \text{where } m = \int_{h_1}^{h_2} \rho \, dy, \quad q = \int_{h_1}^{h_2} \rho u \, dy. \tag{8}$$

The quantities m and q represent respectively the mass density of gas in, and flux of gas through, each cross-section.

As boundary conditions for the temperature we assume that the scroll walls are thermally insulated, so that the normal derivative of T is zero, that is

$$\frac{\partial T}{\partial y} = \frac{\partial h_i}{\partial x}\frac{\partial T}{\partial x} \text{ on } y = h_i(x,t); \quad i = 1, 2. \tag{9}$$

We also have to match the solution in the gap with the prescribed pressure in the chamber on either side:

$$p \to P_1 \text{ as } x \to -\infty, \quad p \to P_2 \text{ as } x \to +\infty. \tag{10}$$

2.2 Dimensionless parameters

Now we compare the sizes of the different terms in equations (1–6) to see what simplifications can be made. Typical values for the physical parameters in the problem are given in table 1. First we note that the geometry is very slender: the gap is typically much longer than it is thick. This feature is chacterised by the *slenderness parameter*,

$$\epsilon = \frac{d}{L} \approx 10^{-4}, \tag{11}$$

and the fact that this is very small will enable us to use *lubrication theory*: a great simplification of the Navier-Stokes equations.

Now, given the pressure drop ΔP across the gap we can deduce a typical gas velocity U by balancing the pressure gradient with viscous drag in (2):

$$U = \frac{d^2 \Delta P}{\mu L}.$$

Another dimensionless parameter is the ratio between this and the velocity due to rotation of the compressor:

$$\Omega = \frac{\omega L}{U} = \frac{\mu \omega L^2}{d^2 \Delta P} \approx 5 \times 10^{-2}. \tag{12}$$

In general the gas flow can be decomposed into (*i*) a "Couette flow" caused by relative tangential motion of the walls, (*ii*) a "squeeze film" due to movement of the walls towards or away from each other, and (*iii*) a "Poiseiulle flow" in which gas is forced through the gap by the imposed pressure difference. If, as appears to be the case, Ω is small, this says that (*iii*) dominates over (*i*) and (*ii*).

Now, using U as the velocity scale we compare the left- and right-hand sides of (2) to determine the importance of inertia in the problem. As usual in lubrication-type problems, the corresponding dimensionless parameter is the *reduced Reynolds number*, which is the classical Reynolds number reduced by a factor of ϵ^2:

$$\mathrm{Re}^* = \frac{\bar{\rho} U L \epsilon^2}{\mu} = \frac{\bar{\rho} d^4 \Delta P}{\mu^2 L^2} \approx 10^{-4}. \tag{13}$$

Since Re^* is small, viscous effects dominate inertia, that is the left-hand side of (2) can safely be neglected.[1]

Similarly, we compare the left- and right-hand sides of (6) using the *reduced Peclet number*:

$$\mathrm{Pe}^* = \frac{\bar{\rho} c_v U L \epsilon^2}{k} = \frac{\bar{\rho} c_v d^4 \Delta P}{\mu k L^2} \approx 10^{-4}.$$

It is no accident that $\mathrm{Pe}^* \approx \mathrm{Re}^*$ since their ratio, the Prandtl number $\mathrm{Pr} = k/(\mu c_v)$, is close to unity for air.

We can immediately deduce a typical rate of leakage from the velocity scale U. The rate at which gas is lost through the channel is of order Ud, and so the cumulative loss over a cycle is typically Ud/ω. We simply have to compare this with the original area of a chamber to obtain the relative loss of gas due to leakage:

$$\text{relative loss} = \frac{d^3 \Delta P}{\mu \omega L^3} = \frac{\epsilon}{\Omega}. \tag{14}$$

The values given in table 1 suggest that this is rather small: about 0.2%. However, it is clearly highly sensitive to increases in d, and if we set $d = 8\,\mu$m, then the typical relative loss is dramatically increased to around 100%. This is in encouraging agreement with the experimental observations noted earlier.

[1] We can also interpret Re^* as the square of a typical Mach number:

$$\mathrm{Re}^* = \frac{U^2}{c^2}, \quad \text{where } c^2 = \frac{\Delta P}{\bar{\rho}},$$

and hence deduce that the flow is wholly subsonic.

2.3 Dimensionless equations

In nondimensionalising the equations (1–6) we utilise the slenderness of the geometry and the difference between the velocity scales for the gas and for the compressor. Thus we set

$$\begin{gathered} x = L\,x', \quad y = d\,y', \quad u = U u', \quad v = \epsilon U v', \quad t = t'/\omega, \\ h_i = d\,h_i', \quad u_i = \omega L\,u_i', \quad p = \Delta P\,p', \quad \rho = \bar{\rho}\,\rho', \quad T = \Delta P\,T'/(\bar{\rho} c_v). \end{gathered} \tag{15}$$

Henceforth we drop the primes and proceed with the dimensionless variables. The Navier-Stokes equations (2), up to order Re^* and ϵ^2, reduce to the *lubrication equations* (see [4])

$$p_y = 0, \quad u_{yy} = p_x. \tag{16}$$

Thus,

$$u = \frac{p_x}{2} y^2 + Ay + B, \tag{17}$$

for some $A(x,t)$, $B(x,t)$, found using the dimensionless version of (7) to be given by

$$A = \frac{\Omega(u_2 - u_1)}{h} - \frac{p_x(h_1 + h_2)}{2}, \quad B = \frac{\Omega(h_2 u_1 - h_1 u_2)}{h} + \frac{p_x h_1 h_2}{2}, \tag{18}$$

where h is the gap thickness:

$$h = h_2 - h_1.$$

Now consider the dimensionless version of the energy equation (6) and thermal boundary condition (9), taking only the terms at leading order in ϵ:

$$\begin{aligned} \frac{1}{\gamma - 1}\left(\Omega p_t + u p_x + v p_y\right) - \frac{\gamma}{\gamma - 1}\frac{p}{\rho}\left(\Omega \rho_t + u \rho_x + v \rho_y\right) - u_y^2 + O(\epsilon^2) \\ = \frac{1}{\mathrm{Pe}^*}\left(T_{yy} + O(\epsilon^2)\right), \end{aligned} \tag{19}$$

$$T_y = O(\epsilon^2) \quad \text{on } y = h_1, h_2. \tag{20}$$

Now we use the fact that Pe^* is much smaller than one to expand T as an asymptotic expansion in powers of Pe^*:

$$T = T_0 + \mathrm{Pe}^* T_1 + \ldots.$$

Notice that, since $\epsilon^2 \ll \mathrm{Pe}^*$, it makes sense to keep terms of order Pe^* while neglecting those of order ϵ^2.

To lowest order in Pe^*, (19, 20) reduces to the trivial homogeneous Neumann problem

$$\frac{\partial^2 T_0}{\partial y^2} = 0, \quad \frac{\partial T_0}{\partial y} = 0 \text{ on } y = h_1, h_2, \tag{21}$$

from which we can deduce only that T_0 is independent of y. But from (16) we know that p is also independent of y, and thus (5) implies that ρ must likewise be a function only of x and t to lowest order.

We can obtain no more information about the functions $p(x,t)$ and $\rho(x,t)$ from the leading-order problem (21). This situation, where the leading-order problem admits nonunique solutions, arises quite often. The way to resolve the nonuniqueness is to proceed to higher order in Pe^* and consider the problem for T_1, namely[2]

$$\frac{\partial^2 T_1}{\partial y^2} = \frac{1}{\gamma-1}\left(\Omega p_t + u p_x\right) - \frac{\gamma}{\gamma-1}\frac{p}{\rho}\left(\Omega\rho_t + u\rho_x\right) - u_y^2, \tag{22}$$

$$\frac{\partial T_1}{\partial y} = 0 \quad \text{on } y = h_1, h_2. \tag{23}$$

Now we have an inhomogeneous Neumann problem, which can only admit solutions for T_1 if a *solvability condition* is satisfied. In this case, by integrating (22) with respect to y and applying (23) we obtain the required relation between $p(x,t)$ and $\rho(x,t)$, namely

$$\Omega p_t + \bar{u} p_x - \frac{\gamma p}{\rho}\left(\Omega\rho_t + \bar{u}\rho_x\right) = (\gamma-1)\bar{u_y^2}, \tag{24}$$

where $\bar{\cdot}$ denotes the cross-sectional average:

$$\bar{\cdot} = \frac{1}{h}\int_{h_1}^{h_2} \cdot \, dy.$$

Now we simply substitute in the analytic form (17) of u to obtain

$$\Omega\left(p_t - \frac{\gamma p}{\rho}\rho_t\right) = \frac{\gamma h^2 p_x}{12}\left(p_x - \frac{p}{\rho}\rho_x\right). \tag{25}$$

A second equation linking p and ρ is obtained by substituting (17) into the dimensionless form of (8), the result of which is

$$\Omega(\rho h)_t + q_x = 0, \quad \text{where } q = \frac{\Omega\rho h(u_1+u_2)}{2} - \frac{\rho p_x h^3}{12}. \tag{26}$$

2.4 Solution in the quasi-steady limit

Equations (25, 26) form a closed leading-order system for ρ and p; recall that u_1, u_2 and h are prescribed functions of x and t. They can be simplified further by taking the *quasi-steady limit* $\Omega \to 0$. Then, from (25) we deduce that

$$\frac{\partial}{\partial x}\left(\frac{p}{\rho}\right) = 0, \tag{27}$$

which implies that the gas is *isothermal*. So in (26) we can set $\rho = p/(T(\gamma-1))$ where T is independent of x. Then, by setting $\Omega = 0$ in (26) we find that the flux

$$q = -\frac{h^3 p p_x}{12T(\gamma-1)} \tag{28}$$

[2]Strictly speaking we should expand p, ρ and u in powers of Pe^* also, but for ease of presentation we do not bother; in effect we use p, ρ and u as shorthand for p_0, ρ_0 and u_0.

is a function only of t. Now we simply divide by h^3 and integrate with respect to x from $-\infty$ to $+\infty$, applying the matching conditions (10), to obtain

$$q = \frac{P_1^2 - P_2^2}{24T(\gamma - 1)} \left(\int_{-\infty}^{\infty} \frac{dx}{h^3} \right)^{-1}. \tag{29}$$

This tells us how the flux, *i.e.* the leakage through the gap, depends on the pressure in the chamber on either side and the geometry of the channel.

It is worth emphasising the difference between this *quasi-steady* solution and a steady-state solution in which all the dependent variables are assumed to be independent of t. We have taken a limit in which the time-derivatives in (25, 26) can be neglected, but p and ρ may still depend on t. In particular, in (29) P_1, P_2, T and h can all be expected to be functions of time.[3]

Since the minimum gap thickness is very small, the integral in (29) is dominated by the behaviour of h near its minimum. In a neighbourhood of this point, we can approximate h by a quadratic function, say

$$h = d(t) + \frac{\kappa(t)x^2}{2},$$

where κ is the *difference between the curvatures* of the two channel walls at their closest point. Then

$$\int_{-\infty}^{\infty} \frac{dx}{h^3} = \frac{3\pi}{4d^{5/2}\sqrt{2\kappa}}.$$

3 Conservation equations for the chambers

Now we consider the conservation of mass and energy for a single chamber of gas. Since the Reynolds number on the scale of a chamber is large, it is usual to assume that the gas in each chamber is turbulent and thus well-mixed. Hence we can associate a spatially-uniform temperature $T(t)$ and pressure $P(t)$ with the mass $M(t)$ of gas in the chamber, which has a given volume $V(t)$.

First, note that the ratio of kinetic to thermal energy is of order

$$\frac{\text{kinetic energy}}{\text{thermal energy}} \sim \frac{\bar{\rho}\omega^2 L^2}{\Delta P} = \Omega^2 \mathrm{Re}^* \ll 1.$$

Therefore we neglect kinetic energy throughout, so that the internal energy in the chamber is simply

$$E = Mc_v T. \tag{30}$$

The internal energy is changed due to (see *e.g.* [5]):

- The work done by changes in the volume V of the chamber which, recall, is assumed to be a prescribed function of time. The work done is given by $-P\,dV/dt$.

[3]The quasi-steady limit reflects the fact that they vary only slowly with t: the parameter Ω can be thought of as the ratio of the timescale (L/U) associated with convection in the gas flow to that $(1/\omega)$ over which P_1, P_2, T, *etc.* vary.

- The energy transported into and out of the chamber through the gaps on either side. Assuming the flow through these gaps is adiabatic, the energy transported by a mass flux q is qH, where H is the *enthalpy*, equal to c_pT.
- Dissipation and energy losses to the external environment, which we denote by $\dot{Q}$.

Putting all these together, we obtain

$$\frac{dE}{dt} = -P\frac{dV}{dt} + q_i c_p T_i - q_o c_p T + \dot{Q}, \tag{31}$$

where the subscripts i and o correspond to flow into and out of the chamber respectively. Notice that the temperature of gas flowing out of the chamber is the same as that of the gas in the chamber, T.

Henceforth we neglect $\dot{Q}$, although thermal interaction with the surroundings might be included in a more refined model. Therefore, substituting (30) into (31) and rearranging, we obtain an ordinary differential equation relating P and T:

$$V\frac{dP}{dt} = \gamma R(q_i T_i - q_o T) - \gamma P\frac{dV}{dt}. \tag{32}$$

Next we consider conservation of mass for the chamber. This simply states that the mass change is equal to the flux into the chamber minus that out:

$$\frac{dM}{dt} = q_i - q_o. \tag{33}$$

But $M = \rho V$, where the density ρ is given in terms of P and T by using the equation of state (5). Thus (33) can be rearranged to a second equation relating P and T:

$$\frac{dT}{dt} = \frac{T}{P}\frac{dP}{dt} + \frac{T}{V}\frac{dV}{dt} - \frac{RT^2}{PV}\left(q_i - q_0\right). \tag{34}$$

Now the idea is as follows. Given the pressure P and temperature T in two neighbouring chambers, and the geometry of the gap between them, we can evaluate the flux from one to the other using (29). Then for each chamber we have the two differential equations (32, 34) for P and T, which are coupled to the corresponding equations for the neighbouring chambers by the fluxes q on either side.

4 The coupled problem

The situation is depicted schematically in figure 4. We have a series of chambers, in the n^{th} of which the gas is at pressure P_n and temperature T_n. The flux between the n^{th} and $(n+1)^{\text{th}}$ chamber is denoted by q_n, with the sign convention that $q_n > 0$ if gas flows *from* chamber n *to* chamber $(n+1)$.

From the theory of section 2, we know that in each of the gaps between the chambers the temperature is constant, but the value of that constant is determined by the sign of q: if

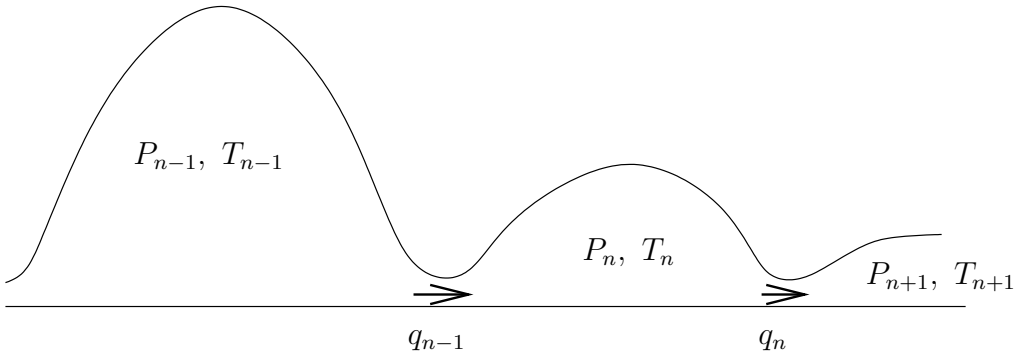

Figure 4: Schematic diagram of the coupling between neighbouring chambers.

$q_n > 0$ then the gas transported by q_n has temperature T_n, while if $q_n < 0$ it is at T_{n+1}. Thus, when we redimensionalise (29) we obtain the following expression for q_n:

$$q_n = \frac{\left(P_n^2 - P_{n+1}^2\right) d^{5/2}\sqrt{\kappa}}{9\pi\sqrt{2}\,\mu R} \begin{cases} 1/T_n & \text{if } P_n > P_{n+1}, \\ 1/T_{n+1} & \text{if } P_n < P_{n+1}. \end{cases} \tag{35}$$

Similarly, when we write down the conservation equations (32, 34) for the n^{th} chamber, whether each of q_{n-1} and q_n qualifies as flux *into* (q_i) or *out of* (q_o) the chamber depends on its sign. The resulting equations can conveniently be written in the form

$$\frac{\dot{P}_n}{P_n} = \frac{\gamma R}{P_n V_n}\left\{q_{n-1}T_n - q_n T_{n+1} + q_{n-1}^+(T_{n-1} - T_n) + q_n^+(T_{n+1} - T_n)\right\} - \frac{\gamma \dot{V}_n}{V_n}, \tag{36}$$

$$\begin{aligned} \frac{\dot{T}_n}{T_n} \;=\; & -\frac{(\gamma-1)\dot{V}_n}{V_n} + \frac{R}{P_n V_n}\left\{q_n T_n - \gamma q_n T_{n+1}\right. \\ & \left. +(\gamma-1)q_{n-1}T_n + \gamma q_{n-1}^+(T_{n-1} - T_n) + \gamma q_n^+(T_{n+1} - T_n)\right\}, \end{aligned} \tag{37}$$

where q^+ denotes the positive part of q:

$$q^+ = \begin{cases} q & \text{if } q > 0, \\ 0 & \text{if } q < 0. \end{cases}$$

To solve the dynamical system (36, 37) we need to apply "end conditions" at the outermost chambers. Suppose there are N chambers altogether, with the first and N^{th} open to reservoirs at *given* pressure and temperature P_0, P_N and T_0, T_N. (Note that T_0 and/or T_N need only be specified if $P_0 > P_1$ and/or $P_N > P_{N-1}$, so that gas flows *into* the adjoining chambers.) We also have to specify P_n and T_n for $n = 1, \ldots, N-1$ at $t = 0$. Finally, there is a complicated closure condition associated with the periodicity of the motion. Roughly speaking, it is clear that after a complete cycle, what was the n^{th} chamber has now become the $(n+1)^{\text{th}}$ chamber. The way in which this condition is implemented in practice should be made clear by the following outlined solution procedure.

1. Suppose P_n and T_n are given at $t = 0$ for $n = 1, \ldots, N$.
2. Integrate the coupled ordinary differential equations (36, 37) forward through one complete cycle, using the specified values of P_0, T_0, P_N, T_N.

3. Set
$$\{V_n,\, P_n,\, T_n\}_{\text{new}} = \{V_{n-1},\, P_{n-1},\, T_{n-1}\}_{\text{old}}\,.$$
4. Go to step 2.

The desired final result is a periodic solution, in which the "new" and "old" values in step 3 above are identical, that is

$$\text{periodic solution} \quad \Rightarrow \quad \{V_n(t),\, P_n(t),\, T_n(t)\} \equiv \{V_{n-1}(t+\tau),\, P_{n-1}(t+\tau),\, T_{n-1}(t+\tau)\}\,,$$

where $\tau = 2\pi/\omega$ is the period of the motion. However, when there is strong coupling between the chambers it is far from clear that this periodic solution is unique or stable. Indeed, for a high-dimensional nonlinear dynamical system such as this, we might expect to see rather complicated dynamics in general.

4.1 The small coupling limit

If the leakage is relatively small (which it should be for any worthwhile compressor), we can perturb about the zero-leakage solution, obtained by solving (36, 37) with $q_n \equiv 0$:[4]

$$P_n = P_0 \left(\frac{V_0}{V_n}\right)^{\gamma}, \quad T_n = T_0 \left(\frac{V_0}{V_n}\right)^{\gamma-1}. \tag{38}$$

Here V_0 is the *choke volume*: the volume of gas ingested by the compressor at the outset of the cycle (the volume marked "1" in figure 1A). Then the lowest-order fluxes are obtained by substituting (38) into the expression (35) for q_n.

Interestingly, if the compressor is in a periodic state, we only need to find q_0 to evaluate the total leakage: in its first cycle, a chamber *gains* $-q_1$ and loses $-q_0$. Then, in the next cycle, it *loses* $-q_1$ and gains $-q_2$. Over the lifetime of a chamber, all the intermediate fluxes cancel each other out, so only q_0 remains. In the small-q limit, this is readily evaluated:

$$-q_0 = \frac{P_0^2 d^{5/2}\sqrt{\kappa}}{9\pi\sqrt{2}\,\mu R T_0} \left(\frac{V_0}{V_1}\right)\left[\left(\frac{V_0}{V_1}\right)^{\gamma} - \left(\frac{V_1}{V_0}\right)^{\gamma}\right]. \tag{39}$$

Thus, assuming that d and the other parameters in (39) are constant (and in any case beyond our control), we obtain a functional form of the total leakage:

$$\text{total leakage} \propto l := \int_0^{\tau} \sqrt{\kappa}\left(\frac{V_0}{V_1}\right)\left[\left(\frac{V_0}{V_1}\right)^{\gamma} - \left(\frac{V_1}{V_0}\right)^{\gamma}\right] dt. \tag{40}$$

We can use this functional as part of a cost function in comparing proposed new compressor designs, for all the variables on the right-hand side of (40) can readily be evaluated for any given scroll geometry. Without performing any detailed calculations, we can immediately deduce some desirable design properties that will reduce leakage:

- The contact should be as *flat* as possible, *i.e.* κ should be minimised.
- The volume should be *reduced gradually on the first cycle*. This follows from the observation that only q_0 is relevant to the total mass loss.

[4] When there is no leakage, the *mass* and *entropy* of the gas in each chamber are preserved: see *e.g.* [5].

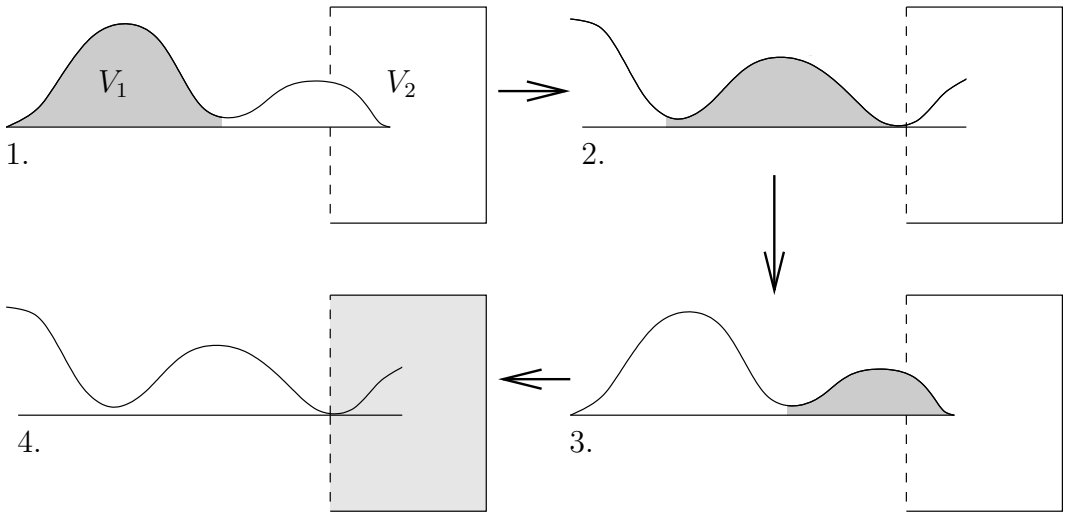

Figure 5: Schematic diagram of the compression of a single chamber (of volume V_1) which opens up into a reservoir of volume V_2.

5 Numerical results

In this section we present some preliminary numerical simulations of the system (36, 37). We consider the simple configuration shown schematically in figure 5. Here, at the beginning of the cycle (diagram 1) the shaded volume of gas V_1 is taken in from the atmosphere. As V_1 decreases (diagram 2) the gas is compressed until the cycle is completed (diagram 3). Then the gas is released into a reservoir of *constant* volume V_2 (diagram 4). The idea is that we run the simulation through several such cycles and see what pressure we can achieve in the reservoir; this seems like a good measure of the efficacy of the compressor.

Equations (36, 37) with q_0 and q_1 given by (35), $q_2 \equiv 0$ and $n = 1, 2$ provide a closed system for P_1, P_2, T_1 and T_2, given the inlet pressure P_0 and temperature T_0. We initiate the calculations with $P_1 = P_2 = P_0$, $T_1 = T_2 = T_0$. As outlined in section 4 at the end of each cycle we perform a replacement algorithm corresponding to (i) a new chamber of atmospheric gas forming in the "new" V_1; (ii) the "old" V_1 discharging into V_2. For the latter we find the new values of P_2 and T_2 by setting the mass and energy in V_2 after the discharge equal to the total mass and energy in V_1 and V_2 immediately prior to the discharge. Thus, after the n^{th} cycle we set

$$\begin{aligned} P_1(n\tau+) &= P_0, \qquad P_2(n\tau+) = \left[\frac{P_1V_1 + P_2V_2}{V_1 + V_2}\right](n\tau-), \\ T_1(n\tau+) &= T_0, \qquad T_2(n\tau+) = \left[\frac{(P_1V_1 + P_2V_2)T_1T_2}{P_1V_1T_1 + P_2V_2T_2}\right](n\tau-). \end{aligned} \tag{41}$$

In all the calculations to follow the parameter values are set as follows,

$$\begin{aligned} \mu = 1, \quad R = 1, \quad \gamma = 1.4, \quad \kappa = 1, \\ P_0 = 1, \quad T_0 = 1, \quad V_2 = 10, \quad \tau = 1, \end{aligned}$$

and we examine the effects of varying the "leakage parameter" d and the form of $V_1(t)$. We

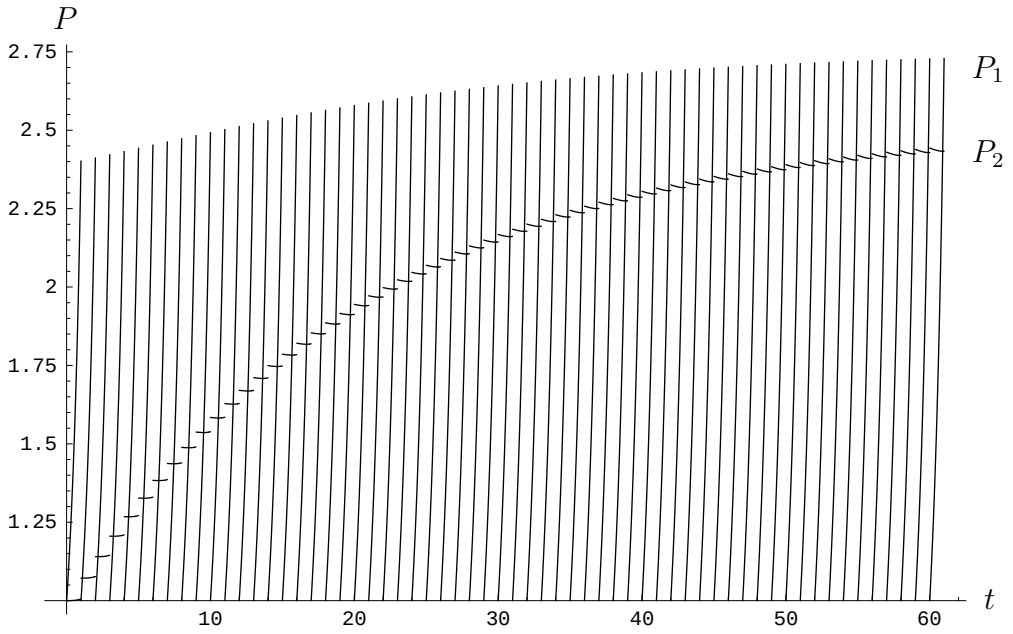

Figure 6: Pressures P_1 (in the compression chamber) and P_2 (in the pressurised reservoir) versus time. The volumes are $V_1 = 1 - 0.5\ t$, $V_2 = 10$ and the leakage parameter $d = 1$.

start with the simplest case in which V_1 is linear in t, say

$$V_1 = 1 - \alpha t,$$

where $\alpha \in (0, 1)$; $\alpha = 0$ implies a compression ratio of one, while as $\alpha \to 1$ the compression ratio goes to infinity. (In [2] it is shown that this linear variation of V_1 with time corresponds to the traditional circle involute design shown in figure 1.)

In figure 6 we plot the pressure in the chamber and the reservoir versus time for the case $\alpha = 0.5$, $d = 1$. We can see how P_1 increases during each cycle and is reset each time a new cycle begins. In the reservoir, P_2 varies only slightly during any cycle, and is incremented gradually at each discharge. Closer examination reveals that, because of leakage between the chamber and the reservoir, P_2 *decreases* when $P_2 > P_1$ and *increases* when $P_2 < P_1$. For these parameter values, the system appears to settle down to a periodic state after around 60 cycles, with the pressure in the reservoir enhanced by a factor of just over 2. From the calculations we can also obtain the temperature variations, but we do not bother to show these as they are irrelevant to the total energy stored in the reservoir, which is proportional to P_2V_2.

In figure 7 we present the corresponding results when $\alpha = 0.8$, so the compression ratio is five, compared with two in the previous calculation. As expected, the increased compression ratio leads to a higher final pressure, although the system also takes somewhat longer to converge to its periodic state.

In the light of figures 6 and 7 it is of interest to ask how the final pressure achieved in the reservoir depends on the compression ratio, *i.e.* on α. As a measure of this we take the

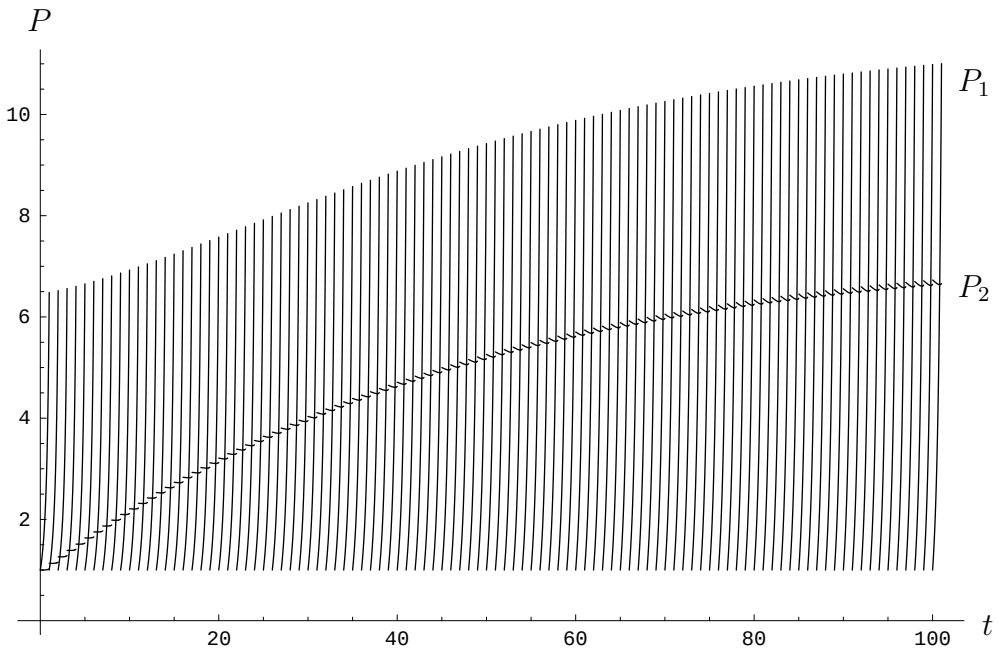

Figure 7: Pressures P_1 (in the compression chamber) and P_2 (in the pressurised reservoir) versus time. The volumes are $V_1 = 1 - 0.8\ t$, $V_2 = 10$ and the leakage parameter $d = 1$.

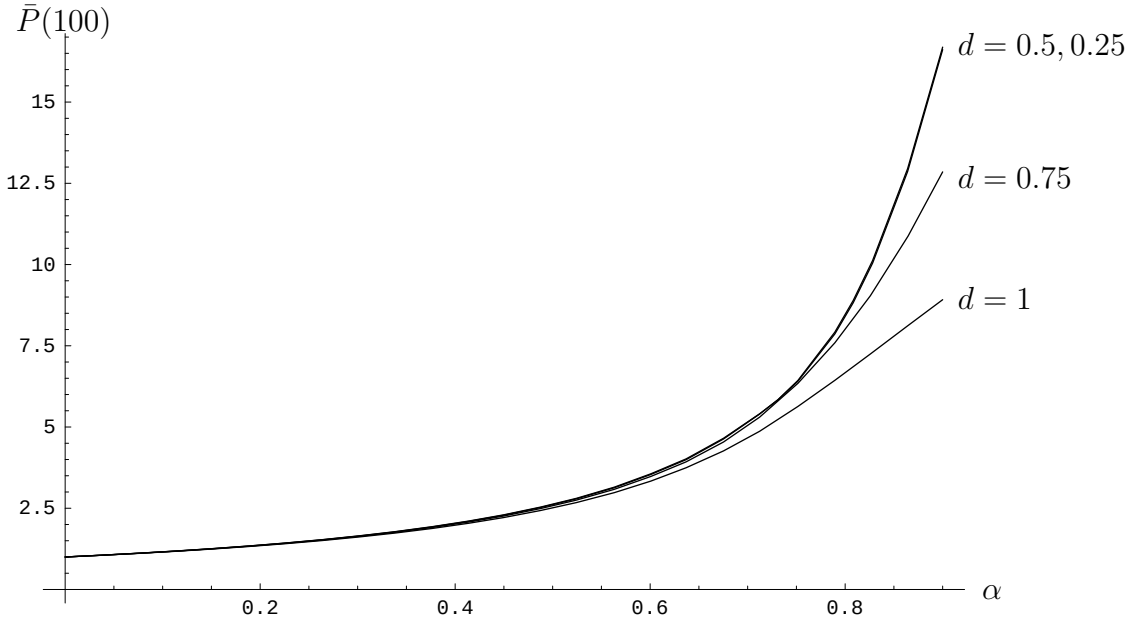

Figure 8: Average reservior pressure over the 100^{th} cycle versus compression parameter α. The volumes are $V_1 = 1 - \alpha t$, $V_2 = 10$ and the leakage parameter $d = 0.25,\ 0.5,\ 0.75,\ 1$. Notice that the curves for $d = 0.25$ and $d = 0.5$ are indistinguishable.

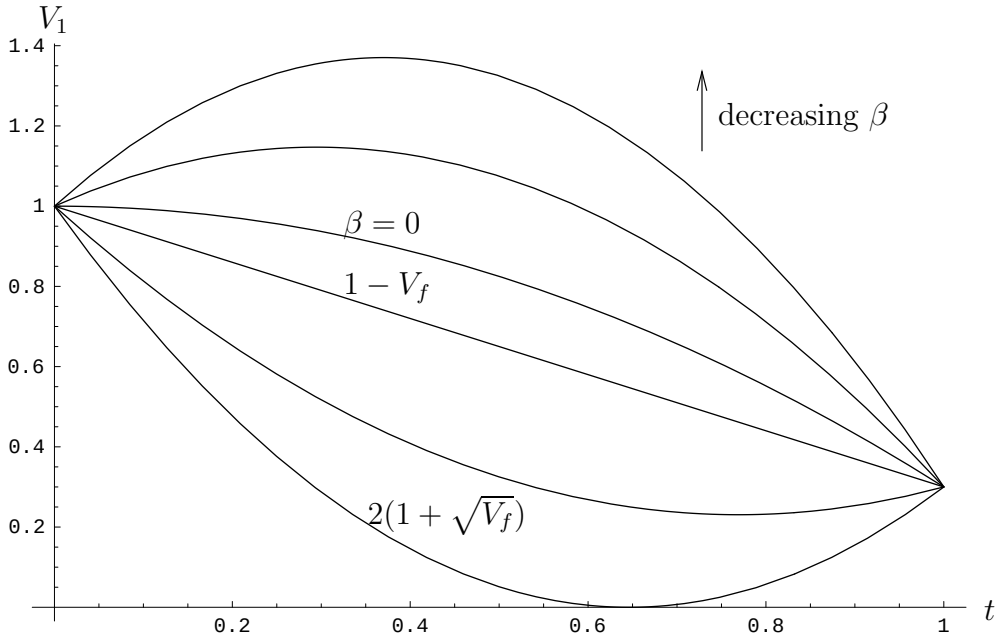

Figure 9: The family of curves $V_1 = 1 - \beta t + (V_f + \beta - 1)t^2$ for various values of β (here $V_f = 0.3$). The value $\beta = 1 - V_f$ gives a straight line joining $V_1 = 1$ at $t = 0$ to $V_1 = V_f$ at $t = 1$; $\beta = 0$ has zero gradient at $t = 0$; $\beta = 2(1 + \sqrt{V_f})$ is the value at which V_1 first reaches zero for $t \in (0, 1)$.

average of P_2 over the 100^{th} cycle:

$$\bar{P}(100) = \int_{100}^{101} P_2 \, dt,$$

and plot the result versus α for various values of d in figure 8. Not surprisingly the pressure achieved increases as α is increased and as d is decreased. However, for sufficiently small d, decreasing d still further doesn't appear to have much effect; the graphs for $d = 0.25$ and $d = 0.5$ are indistinguishable. This is explained by examination of the transients, which makes it clear that for these small values of d, P_2 has yet to equilibriate after 100 cycles.

So, we have shown the rather obvious results that the effectiveness of a compressor can be enhanced by increasing the compression ratio and by reducing the leakage, although these also make the convergence to maximum compression slower. Next we would like to compare compressors with the same compression ratio but different histories $V_1(t)$. Therefore we consider the family

$$V_1 = 1 - \beta t + (V_f + \beta - 1)t^2,$$

shown in figure 9, where V_f is the final volume (so the compression ratio is $1/V_f$) and β changes the volume history for a fixed V_f; $\beta = 1 - V_f$ gives the linear $V_1(t)$, *i.e.* constant compression rate, considered previously. Broadly speaking, if β is decreased the compression is slower initially and accelerates towards the end of the cycle, and vice versa.

First we check how our theoretical approximate leakage l given in (40) varies with β. In figure 10 we plot l versus β for different values of V_f. We observe that the theoretical leakage

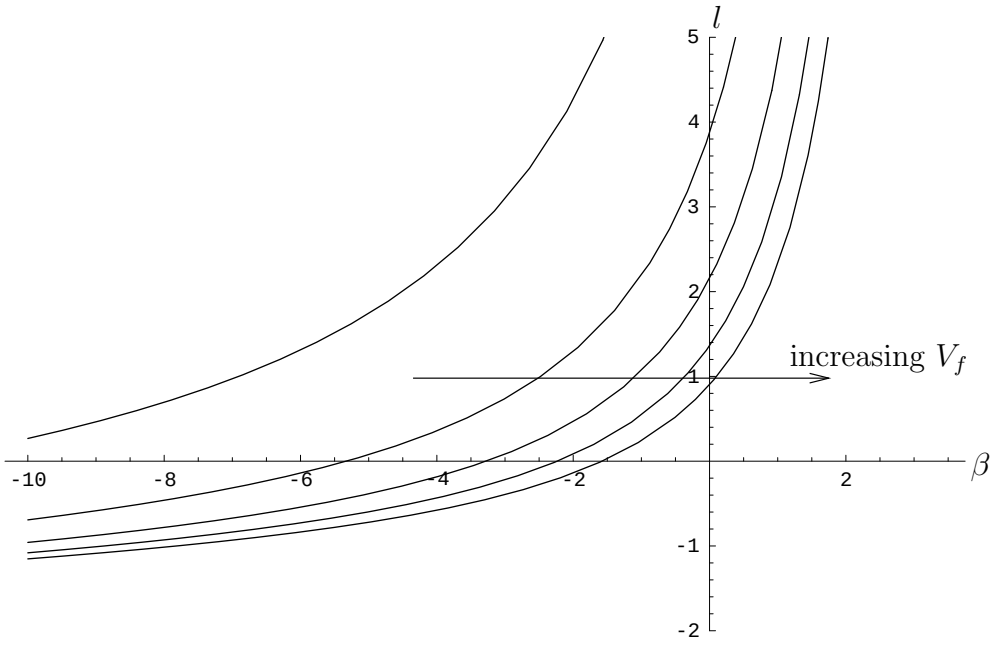

Figure 10: Theoretically predicted leakage $l = \int_0^1 (V_1^{-\gamma-1} - V_1^{\gamma-1})\, dt$ for the family of volume histories depicted in figure 9; $V_1 = 1 - \beta t + (V_f + \beta - 1)t^2$ with $V_f = 0.1$, 0.2, 0.3, 0.4, 0.5.

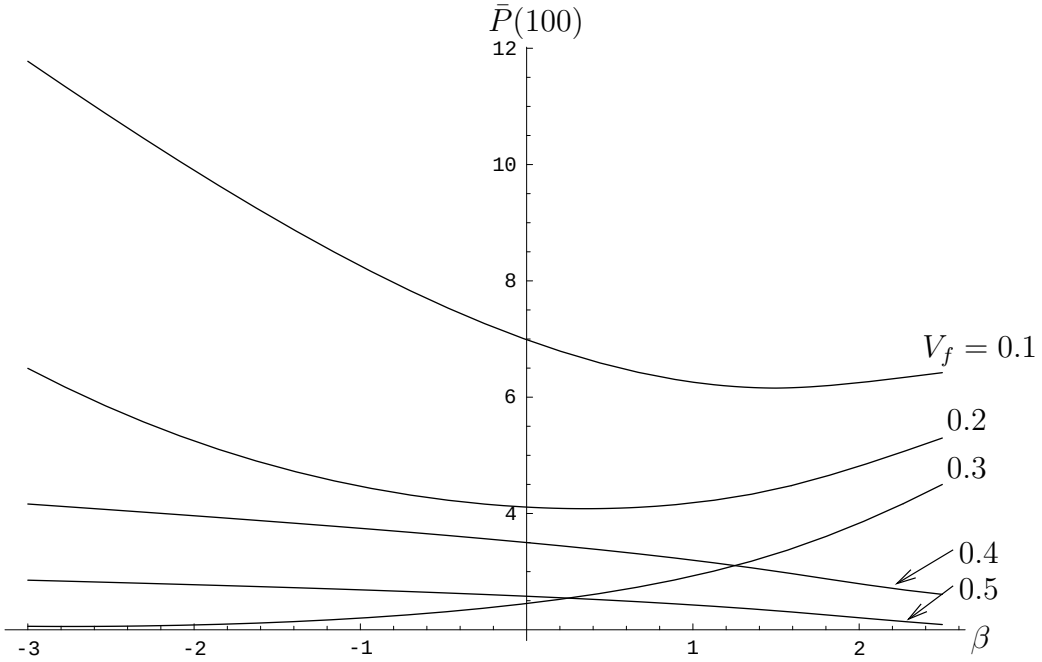

Figure 11: Average reservior pressure over the 100^{th} cycle for $d = 1$ and the family of volume histories depicted in figure 9; $V_1 = 1 - \beta t + (V_f + \beta - 1)t^2$ with $V_f = 0.1$, 0.2, 0.3, 0.4, 0.5.

for a given volume ratio is reduced if the compression is slow at the beginning and faster at the end. This echoes the suggestion at the end of section 4 that the volume should be reduced gradually at the start. There is a surprise, however, in that l can be *negative* if β is sufficiently large and negative. This corresponds to large positive excursions in V_1 (see figure 9), as a result of which the compressor acts like a bellows, sucking extra gas into the chamber.

This conclusion is backed up by figure 11 in which we plot $\bar{P}(100)$ from our simulation versus β for different values of V_f (and with $d = 1$). Here the behaviour in general is extremely interesting: depending on the compression ratio, $\bar{P}$ may be an increasing or decreasing function of β, or may vary nonmonotonically. However, for the large compression ratios which are likely to be of most practical interest, the optimal performance (*i.e.* largest possible value of $\bar{P}(100)$) is obtained by making β as large and negative as possible.

6 Conclusions

Here we summarise the work presented in this case study and suggest some open questions (labelled (a), (b), *etc.*) which the interested reader might consider further.

We have used compressible lubrication theory to obtain a theoretical prediction of the leakage between adjoining chambers in a scroll compressor. One surprising outcome of the analysis is that the gas flowing through the narrow gap between one chamber and the next is *isothermal*. In traditional inviscid gas dynamics one would expect the temperature to decrease as the gas accelerates through the gap, while classical lubrication theory would predict an increase in temperature due to viscous dissipation. Remarkably these two effects appear to cancel each other out exactly.

(a) Is there a simple physical explanation for this result?

Our result for inter-chamber leakage was then incorporated in a coupled model for the pressure and temperature of the gas in each chamber. The model takes the form of a dynamical system.

(b) What can be said about the general properties of the dynamical system (36, 37)? For example, is the desired periodic solution linearly stable?

Our analysis was limited to examination of the case in which the leakage is small. In this limit we obtained an approximate measure of the total losses due to leakage, as a functional of the geometry of the compressor. This could in future be included in a cost function for evaluating proposed new compressor designs.

(c) What other parameters should be included in the cost function? How might an optimisation procedure be implemented?

We performed some numerical simulations of a simple compressor with just one chamber pumping gas into a sealed reservoir. From these we were able to test the effects on compressor performance of varying the leakage rate, the volume ratio and the volume history. The most intriguing possibility suggested by the simulations is that of making the chamber volume *increase* initially, before a rapid compression just prior to discharge. This allows the compressor to use the leakage in its favour by sucking more gas in from the atmosphere.

(d) Is it physically possible to design a scroll for which the chamber volume varies nonmonotonically with time?

Many potentially important physical effects have been neglected in this study, and might be considered in the future to refine the model further.

(e) What would be the effects on our model of including (*i*) thermal losses through the compressor walls; (*ii*) dependence of viscosity upon temperature; (*iii*) the "squeeze film" and "Couette" effects in the lubrication analysis (*i.e.* the terms multiplied by Ω in (25, 26))?

Perhaps most importantly, we have restricted our analysis to a two-dimensional configuration.

(f) How could one quantify leakage through the *sides* of the chambers (*i.e.* in the plane shown in figure 2)?

Finally let us return to the three original questions posed on page 3 and examine the extent to which they have been answered. Although Question 1 has not been adressed in this case study, some progress was made at the Study Group, and in [2] a simple geometric method is given to parametrise a large class of viable compressor spirals. Our modelling provides a framework within which Question 2 can be answered, since different proposed designs can be simulated and their performance and efficiency compared. Moreover, we have proposed some general design strategies which might enhance performance. Finally, in answer to Question 3 we have identified an easily-evaluated functional which measures leakage and could form part of a cost function.

Acknowledgements

I am very grateful to Stig Helmer Jørgensen (DANFOSS) for stimulating my interest in the problem and to the other participants in the Study Group, in particular Jens Gravesen and Christian Henriksen, for useful discussions. I also received some helpful advice from Hilary and John Ockendon.

References

[1] Creux, L. 1905 *Rotary Engine*. US Patent 801182.

[2] Gravesen, J., Henriksen, C. & Howell, P. D. 1998 DANFOSS: Scroll optimization. In *Proceedings of the 32nd European Study Group with Industry*, ed. J. Gravesen & P. G. Hjorth.

[3] McCullough, J. E. & Hirschfeld, F. 1979 The scroll machine — an old principle with a new twist. *Mech. Eng.* **101**(12), 46–51.

[4] Ockendon, H. & Ockendon, J. R. 1995 *Viscous Flow*. Cambridge.

[5] Van Wylen, G. J., Sonntag, R. E. & Borgnakke, C. 1994 *Fundamentals of Classical Thermodynamics*. Wiley.